An infrared spectroscopic comparison of four Chinese palygorskites

Qinfu Liu [a], Xiang Yao [b], Hongfei Cheng [a,b,*], Ray L. Frost [b•]

[a] *School of Geoscience and Surveying Engineering, China University of Mining & Technology, Beijing, 100083 China*

[b] *School of Chemistry, Physics and Mechanical Engineering, Science and Engineering Faculty, Queensland University of Technology, 2 George Street, GPO Box 2434, Brisbane, Queensland 4001, Australia*

Abstract

Infrared spectroscopy has been used to characterize and compare four palygorskite mineral samples from China. The position of the main bands identified by infrared spectra is similar, but there are some differences in intensity, which are significant. In addition, several additional bands are observed in the spectra of palygorskite and their impurities. This variability is attributed to differences in the geological environment, such as the degree of weathering and the extent of transportation of the minerals during formation or deposition, and the impurity content in these palygorskites. The bands of water and hydroxyl groups in these spectra of palygorskite samples have been studied. The characteristic band of palygorskite is observed at 1195 cm^{-1}. Another four bands observed at 3480, 3380, 3266 and 3190 cm^{-1} are attributed to the water molecules in the palygorskite structure. These results suggest that the infrared spectra of palygorskites mineral from different regions are decided not only by the main physicochemical properties of palygorskite, but also by the amount and kind of impurities.

Keywords: Infrared spectroscopy; sepiolite, Palygorskite; Carbonate; Clay

• Corresponding authors.
E-mail addresses: hongfei.cheng@qut.edu.au (H. Cheng), r.frost@qut.edu.au (R. L. Frost)

1. Introduction

Palygorskite, with the ideal chemical composition $MgAlSi_4O_{10}(OH)_4 \cdot H_2O$, is a crystalline hydrated magnesium silicate with a fibrous morphology. Strictly the formula is for sepiolite. Upon substitution of the Mg by for example Fe, then the term palygorskite is used. Palygorskite is known to form a continuous two dimensional tetrahedral sheet, but differs from other layered silicates in lacking continuous octahedral sheets [1]. Palygorskite and sepiolite are fibrous clay minerals reported in soils of arid and semi-arid regions [2]. The structure of palygorskite contains ribbons of 2:1 phyllosilicates linked by periodic inversion of the apical oxygens of the continuous tetrahedral sheet every six atoms of Si (three tetrahedral chains) for sepiolite and every four atoms of Si (two tetrahedral chains) for palygorskite. The tetrahedral sheet is continuous across ribbons but the octahedral sheet is discontinuous as a result of the periodic inversion, and terminal octahedral cations must complete their coordination sphere with water molecules referred to as coordinated water [3, 4].

Palygorskite is widely applied in many fields of material industry, particularly as oil refining, wastewater treatment, removal of odor, drug, and pesticide carriers, catalysts, paper and detergent industries [5-8]. This mineral has some particularly desirable sorptive, colloidal-rheological and catalytic properties, in comparison with other clay minerals [9]. At the same time, palygorskite can form with organic compounds complexes of hydrophobic properties (so called organoclays) [10]. Technological applications are based on its physicochemical, principally on structure, composition, thermal behavior, surface area, among others, and especially in the structure and thermal stability. In general, the industrial raw palygorskite is a mixture of minerals, which contains different mineral impurities as well as major and minor clay minerals. The palygorskite clays from China with the major clay mineral palygorskite include minor carbonates including dolomite and calcite as non-clay minerals. Therefore, it is of great interest to undertake a comparative study of palygorskites from China.

Although the extensive use of palygorskite in industrial processes and its excellent characteristics for the preparation of organic/inorganic complexes, there is little

information about the structural analysis of palygorskite, especially Chinese palygorskites and their impurities. It is noteworthy that there is a certain variability in the formula and structure of palygorskite due to the influence of isomorphic substitution and various geological environments in different region. The aim of this work is to study how impurities and geological environment influence the position and intensity of the vibrations of the infrared spectra. Therefore, infrared spectroscopy study has been carried out on four Chinese palygorskites. By this means, valuable information can be obtained and infrared spectroscopy can be used to analysis palygorskite and differentiate the impurities.

2. Experimental methods

2.1 Materials

Four palygorskite samples, containing impurities quartz and dolomite, were selected for this study (Table 1). The samples were used directly, without prior size fraction separation, since one of the objectives was to determine the influence on the thermal behavior of mineral samples.

2.2 X-ray diffraction

X-ray diffraction patterns were collected using a PANalytical X'Pert PRO X-ray diffractometer (radius: 240.0 mm). Incident X-ray radiation was produced from a line focused PW3373/10 Cu X-ray tube, operating at 40 kV and 40 mA, with Cu Kα radiation of 1.540596 Å. The incident beam passed through a 0.04 rad soller slit, a 1/2 ° divergence slit, a 15 mm fixed mask, and a 1 ° fixed antiscatter slit.

2.3 Infrared spectroscopy

Infrared spectra were obtained using a Nicolet Nexus 870 FTIR spectrometer with a smart endurance single bounce diamond ATR cell. Spectra over the 4000-500 cm^{-1} range were obtained by the co-addition of 64 scans with a resolution of 4 cm^{-1} and a mirror velocity of 0.6329 cm/s. Spectra were co-added to improve the signal to noise ratio. No sample preparation was involved.

Band component analysis was undertaken using the Jandel'Peakfit'(Erkrath, Germany) software package which enabled the type of fitting function to be selected and allowed specific parameters to be fixed or varied accordingly. Band fitting was done using a Lorentz-Gauss cross-product function with the minimum number of component bands used for the fitting process. The Lorentz-Gauss ratio was maintained at values greater than 0.7 and fitting was undertaken until reproducible results were obtained with squared correlations (r^2) greater than 0.998. Band fitting of the spectra is quite reliable providing there is some band separation or changes in the spectral profile.

3. Results and discussion

3.1 X-ray diffraction (XRD)

The XRD patterns of the four selected palygorskite minerals with standard XRD patterns are shown in Fig.1. These patterns show that the mineral compositions within these four palygorskite samples are various, and the notable difference between these samples is the occurrence of some impurities. Three sharp strong reflections at 2θ=8.32, 26.62 and 30.86 are due to the palygorskite (P), Quartz (Q) and dolomite (D). The XRD patterns of these representative palygorskite samples from four different regions in China show that quartz is ubiquitous throughout these four samples, with slight variations in relative proportions. Samples I-1 and Z-1 contain significant amounts of dolomite. The XRD patterns of representative clay separates of these four samples reveal that these four samples have similar clay mineral compositions, consisting mainly of palygorskite. These four samples consist mainly of palygorskite. Changes in the phase compositions of the clay minerals and of the palygorskite crystallinity are seen from Fig.1. It is found that palygorskite sample F-1 and G-1 are pure and more crystalline than the others. This variability may be attributed to differences in the geological environment such as degree of weathering or the extent of transportation of the minerals during formation or deposition [11].

3.2 Infrared spectroscopy

The infrared spectra of four Chinese palygorskites are shown in Fig. 2. The results of the band component analysis of the infrared spectra and the band assignments are reported in Table 2. The spectral differences and band component analysis are found to be very useful in order to differentiate these palygorskites from different origins and their chemical composition. Fig. 2 illustrates the infrared spectra of palygorskite from Feidong, Anhui province of China in comparison to that from other areas. Some variations in both the band positions and intensities of the OH, Si–O group vibrational modes and some impurities among these four palygorskites are observed. For convenience, the infrared spectra of these four palygorskites are divided into three sections; these are (a) the 3750-2750 cm^{-1} region attributed to OH and Si-OH stretching vibration modes (Fig. 3); (b) the 1750-1250 cm^{-1} region due to the impurities and water molecule in the structure of palygorskite (Fig. 4) and (c) the 1250-750 cm^{-1} region (Fig. 5).

3.2.1 3750-2750 cm^{-1} region

The infrared spectra of four palygorskites in the 3750-2750 cm^{-1} region are shown in Fig. 3. The IR wavenumbers of palygorskites framework bands, obtained band component analyses are given in Table 1. In the higher wavenumber region of the samples studied the following bands can be observed (Fig. 3):

(1) Three sharp peak or shoulder at 3620, 3580 and 3550 cm^{-1}

(2) Four bands centered at 3480, 3380, 3266 and 3190 cm^{-1}

These three bands observed at 3620, 3580 and 3550 cm^{-1} are in good agreement with the work from Frost *et al.*, apart from an additional band at 3720 cm^{-1} for I-1 [12] and these three bands seem to be characteristic of this mineral. It is probable that differences in the band positions may arise from variations in the mineral composition, sample dryness, sample origin, impurities and sample preparation for spectroscopic analysis. Further, the fitting of a base line and the band component analysis will alter the position of the peaks compared with those, which are read directly from the raw spectra. It is concluded that the band at 3620 cm^{-1} must be ascribed to bonds located in “inaccessible positions” in palygorskite, therefore must be related to $2M_2$-OH bonds. It is well

established in the literature that this is due to the OH stretching modes in the Al_2-OH group [9, 13]. This band has been found in these four samples here studied, but with different intensities. According Chahi [14] and Frost *et al.* [12], the bands at 3580 and 3550 cm^{-1}, based on comparison with smectite, are attributed to the symmetric and antisymmetric stretching modes of Al-Fe^{3+}-OH or Al-Mg-OH band.

With respect to the four bands centered at 3480, 3380, 3266 and 3190 cm^{-1}, as can be seen in Fig. 3, these five samples here studied are similar in position but not in intensity. As reported by Frost *et al.* [15] and Suarez [16], in the structure of palygorskite, four water molecules are bonded to the Mg^{2+} cations at the both ends of each ribbon and located in the nanopores. These molecules are called bound (structural or crystal) water in palygorskite. Furthermore, four water molecules per half-unit cell are located two per two with in the nanocahannels in both sides of each other ribbon. These water molecules are in hydrogen bonding with bound water and are called zeolitic water. Therefore, these bands observed at 3480, 3380, 3266 and 3190 cm^{-1} are due to water molecules in the palygorskite structure. These also are in good agreement with the literature recording the assignation at water molecules (coordinated and zeolitic water) [9, 12, 17].

Changes in the mineral composition of these four palygorskites result in different IR spectra. In general, seven bands discussed above in this spectral region for palygorskite seem to be characteristic of this mineral. These bands studied here are similar in position but not in intensity. This variability may be attributed to differences in the geological environment, such as intensity of weathering or the extent of transportation of the minerals during formation or deposition, and the content of impurity. Comparing these four palygorskite minerals, both F-1 and G-1, with minor impurity quartz, show the typical bands as above. However, palygorskites, regardless of the content of mainly composition, exhibited several additional bands of the spectrum for the palygorskite mineral F-1. This may be due to the existence of impurity. In the spectrum of I-1, an additional band at 3720 cm^{-1} are attributed to hydroxyls attached to the tetrahedral silicon in the palygorskite structure. It is suggested that this band is the non-hydrogen bonded hydroxyl group on the tetrahedral silicate minerals including the layered silicates and

zeolites, and is assigned to terminal Si-OH group. The band observed at 3656 cm^{-1} is assigned to the OH stretching vibration mode of M-OH. As reported by Frost *et al.* [18], these two bands are common in the spectra of attapulgite. One possible reason is that differences in the physico-chemical conditions during the weathering process from different geographical regions. These results suggest that the infrared spectrum of palygorskite mineral from different region is decided not only by the main physicochemical composition of palygorskite, but also by the amount and kind of impurities.

3.2.2 1750-1250 cm^{-1} region

The infrared spectra in the 1750 to 1250 cm^{-1} for these four palygorskites are shown in Fig. 4. In this region of these four palygorskites studied two sections can be observed. They are: (1) Two bands centered at 1658 and 1630 cm^{-1}, which appear in all samples; (2) A shoulder centered at 1457 cm^{-1}, which appears in the samples I-1 and Z-1. It is reported that the presence of two partially resolved bands at 1658 and 1630, which correspond to bending modes of absorbed and zeolitic water. The band observed at 1658 cm^{-1} is attributed to water that is very strongly bound, as would be expected from water coordinated to the magnesium. The 1630 cm^{-1} band is attributed to the adsorbed or surface water [18]. This result is consistent with the results discussed above. With respect to the bands centered at 1485, 1457 and 1400 cm^{-1}, as can be seen in Fig.4, the samples I-1 and Z-1 studied are similar in position but not in intensity. These three bands are assigned to the $(CO_3)^{2-}$ antisymmetric stretching modes [19].

A comparison of Fig. 4 gives some understanding that not only the bending modes of absorbed and zeolitic water are observed, but also the $(CO3)^{2-}$ antisymmetric and symmetric stretching modes also appeared. It is thus evident that there are some impurities in the samples I-1 and Z-1, this result is in good agreement with XRD patterns, thus suggesting for successful application of these palygorskites, impurities such as carbonate and sulfate that were not removed during mining must be removed from palygorskite by chemical treatment before it can be further processed.

3.2.3 1250-750 cm^{-1} region

Fig. 5 shows the IR spectra of the four Chinese palygorskites in 1250-750 cm^{-1} region. Between 1250 and 700 cm^{-1} characteristic bands of silicate can be observed, mainly those corresponding to Si-O bonds in the tetrahedral sheet, and also to M-O stretching vibrational bands. This interval of wavenumber is complex because the lattice modes and the mount and kind of impurities also have some influence in this region of spectra [9]. Therefore, it is important to note that the spectra in this region not only provide the information about the nature of the octahedral sheet, but also display the characteristic bands of OH deformation.

According to the research by Frost *et al.* [12], the bands between 1160 and 1115 cm^{-1} are assigned to Si-O stretching modes and those between 986 and 700 cm^{-1} are attributed to M-OH deformation. However, when the spectra of the Chinese samples are compared, some important differences may be observed. This may be due to the existence of impurity, various physico-chemical conditions and geological environment in different regions. The spectra in this region of all samples, the most intense bands centered at 980 and 1030 $cm^{-1}$are assigned to deformation vibration of OH and stretching of the Si-O bond, which are similar in position and intensity in all samples. Another band at 1126 cm^{-1} corresponds to the stretching of the Si-O band. The characteristic band of palygorskite is observed at 1195 cm^{-1}, which is in good agreement with the research by Suarez [9]. The band centered at 910 cm^{-1} in all samples is observed, which is assigned to the Al-OH-Al deformation, and it is a consequence of the dioctahedral character of palygorskite [14, 20]. The band centered at 875 cm^{-1} is attributed to vibrational modes of band Al-Fe-OH [14]. Another band at 1095 cm^{-1} is observed in all samples. One possible assignment of this band is to the stretching vibration of Si-O antisymmetric stretching mode.

In general, six bands discussed above for palygorskite which seem to be characteristic of this mineral. These bands studied here are similar in position and intensity. Comparing these four palygorskite minerals, both F-1 and G-1, with minor impurity quartz, show the typical bands as above. This result is consistent with the

discussion, above. On the other hand, there are some additional bands appearing, especially in samples I-1 and Z-1. This is because palygorskite in sediments is often found mixed with some carbonate, silicates and to a lesser degree with organic matter. This is attributed to the early digenetic origin of palygorskite by transformation of other minerals.

4. Conclusions

Infrared spectroscopy is used to study the difference in the structure among four Chinese palygorskites. Water and hydroxyl groups in these palygorskite samples have been studied. Several types of water molecules were observed in this mineral. Some differences are found in the XRD results. A remarkable difference in the hydroxyl groups and water was observed by infrared spectroscopy.

The infrared spectra showed hydroxyl stretching at 3620, 3580 and 3550 cm^{-1} for the palygorskite and at 3480, 3380, 3266 and 3190 cm^{-1} for the water in the structure of palygorskite. Six bands were observed between 1250 and 750 cm^{-1} region. These bands are the basic structure of palygorskite. There are some differences among these four Chinese palygorskite. This discrepancy may be attributed to various physico-chemical conditions and geological environment in different region and the existence of impurity. Therefore, impurities such as carbonate and sulfate that were not removed during mining must be removed from palygorskite by chemical treatment before it can be further processed.

Acknowledgment

The authors gratefully acknowledge the financial support provided by the National Natural Science Foundation of China (51034006) and China Postdoctoral Science Foundation funded project (2011M500034). The infra-structure support of the School of Chemistry, Physics and Mechanical Engineering, Science and Engineering Faculty is thanked.

References

[1] N. Frini-Srasra, E. Srasra, Desalination 250 (2010) 26.

[2] M. Shirvani, F. Nourbakhsh, Appl. Clay. Sci. 48 (2010) 393.

[3] E. Garcia-Romero, M. Suarez, Clay Clay Miner. 58 (2010) 1.

[4] H. Cheng, J. Yang, R.L. Frost, Z. Wu, Spectrochim. Acta A 83 (2011) 518.

[5] M.E. Sedaghat, M. Ghiaci, H. Aghaei, S. Soleimanian-Zad, Appl. Clay Sci. 46 (2009) 131.

[6] M. Onal, Y. Sarikaya, Appl. Clay Sci. 44 (2009) 161.

[7] S. Kocaoba, Desalination 244 (2009) 24.

[8] Z.-Q. Lei, S.-X. Wen, Eur. Polym. J. 44 (2008) 2845.

[9] M. Suarez, E. Garcia-Romero, Appl. Clay Sci. 31 (2006) 154.

[10] H.H. Murray, Clay Miner 34 (1999) 39.

[11] C.S. Manju, V.N. Nair, M. Lalithambika, Clay Clay Miner. 49 (2001) 355.

[12] R.L. Frost, O.B. Locos, H. Ruan, J.T. Kloprogge, Vib. Spectrosc. 27 (2001) 1.

[13] C. Blanco, F. González, C. Pesquera, I. Benito, S. Mendioroz, J.A. Pajares, Spectrosc. Lett. 22 (1989) 659

[14] A. Chahi, S. Petit, A. Decarreau, Clay Clay Miner. 50 (2002) 306.

[15] R.L. Frost, J. Kristof, Z. Ding, E. Horvath, 2001 a Clay Odyssey, Proceedings of the International Clay Conference, 12th, Bahia Blanca, Argentina, July 22-28, 2001 (2003) 523.

[16] M. Suarez, E. Garcia-Romero, M.S. del Rio, P. Martinetto, E. Dooryhee, Clay Miner. 42 (2007) 287.

[17] H. Cheng, J. Yang, R.L. Frost, Thermochim. Acta 512 (2011) 202.

[18] R.L. Frost, G.A. Cash, J.T. Kloprogge, Vib. Spectrosc. 16 (1998) 173.

269 [19] R.L. Frost, S. Bahfenne, J. Graham, Spectrochim. Acta A 71 (2008) 1610.

270 [20] J. Madejová, P. Komadel, Clay Clay Miner. 49 (2001) 410.

271

LIST OF TABLES

Table 1 Palygorskite samples from China

Table 2 Infrared absorption bands of palygorskites as obtained from band component analysis

Table 1

Palygorskite Samples	Location	Content of clay mineral	Impurities
Palygorskite(F-1)	Feidong, Anhui province of China	Palygorskite	Quartz
Palygorskite(G-1)	Guanshan, Anhui province of China	Palygorskite	Quartz
Palygorskite(I-1)	Inner Mongolia of China	Palygorskite	Quartz, Dolomite
Palygorskite(Z-1)	Zhangze, Jiangsu province of China	Palygorskite	Quartz, Dolomite

Table 2 Infrared absorption bands of palygorskites as obtained from band component analysis

Samples	Palygorskite (F-1)	Palygorskite (G-1)	Palygorskite (I-1)	Palygorskite (Z-1)	Suggested assignments
			3702		SiOH-stretch
			3656		MgOH-stretch
	3627	3630	3621	3627	OH-stretch
	3612	3614		3615	OH-stretch
	3590	3580	3583	3587	OH-stretch
	3575	3550	3558	3550	OH-stretch
	3544				
	3517				
	3478	3480	3481	3490	Water OH-stretch
	3380	3378	3378	3382	Water OH-stretch
	3266	3266	3253	3266	Water OH-stretch
	3197	3171	3182	3194	Water OH-stretch
	1679				
	1656	1658	1646	1660	Water OH bend
	1631	1628		1629	Water OH bend
			1485	1486	Caronate impurity
			1457	1454	Caronate impurity
			1400	1400	Caronate impurity
	1195	1195	1195	1195	
	1126	1126	1126	1126	SiO stretch
	1097	1097	1095	1093	M-O stretch
	1033	1030	1028	1029	SiO stretch
	985	980	981	980	OH deformation
	973				OH deformation
	943	941	933	944	AL-OH deformation
	912	912	908	908	OH deformation
	879	879	873	879	Al-Fe-OH deformation
			800		

LIST OF FIGURES

Fig.1 XRD patterns for palygorskite samples (a) F-1, (b) G-1, (c) I-1, (d) Z-1

Fig.2 Infrared spectra of Chinese palygorskites of (a) F-1, (b) G-1, (c) I-1, (d) Z-1

Fig.3 Infrared spectra of Chinese palygorskites of (a) F-1, (b) G-1, (c) I-1, (d) Z-1 in 3750-2750 cm^{-1}

Fig.4 Infrared spectra of Chinese palygorskites of (a) F-1, (b) G-1, (c) I-1, (d) Z-1 in 1750-1250 cm^{-1}

Fig.5 Infrared spectra of Chinese palygorskites of (a) F-1, (b) G-1, (c) I-1, (d) Z-1 in 1250-750cm^{-1}

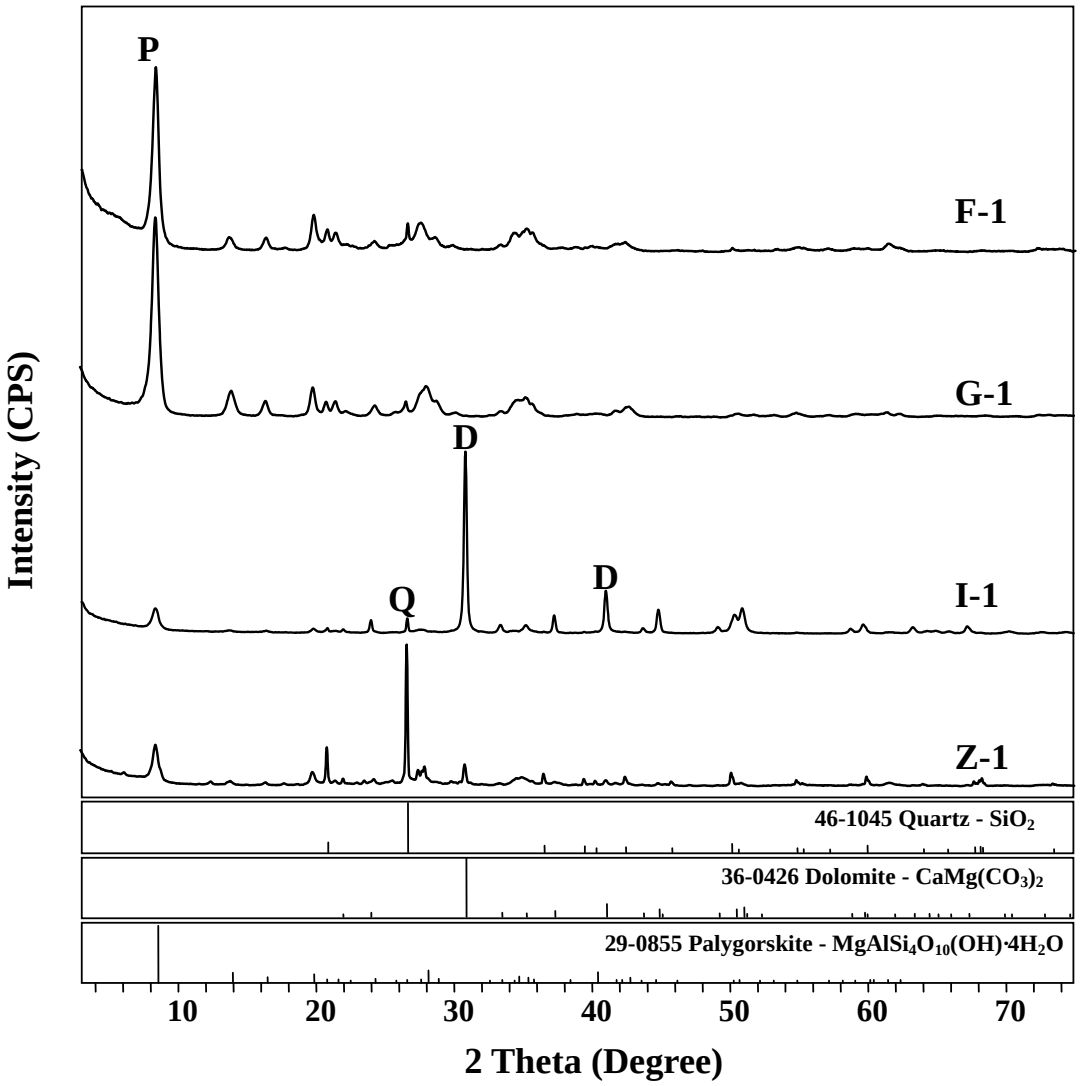
P
F-1
G-1
D
D
Q
I-1
Z-1
Intensity (CPS)
46-1045 Quartz - SiO2
36-0426 Dolomite - CaMg(CO3)2
29-0855 Palygorskite - MgAlSi4O10(OH)·4H2O
10
20
30
40
50
60
70
2 Theta (Degree)

Fig.1

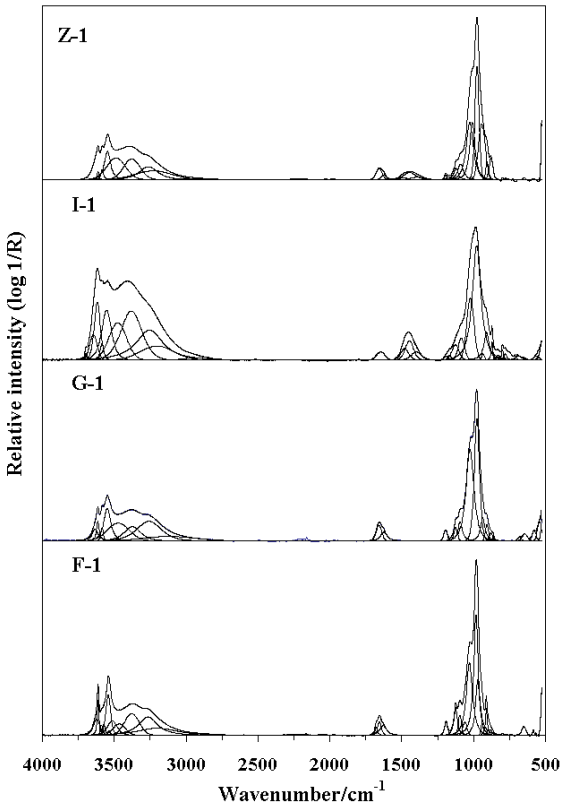
Z-1
I-1
G-1
F-1
Relative intensity (log 1/R)
4000
3500
3000
2500
2000
1500
1000
500
Wavenumber/cm-1

Fig.2

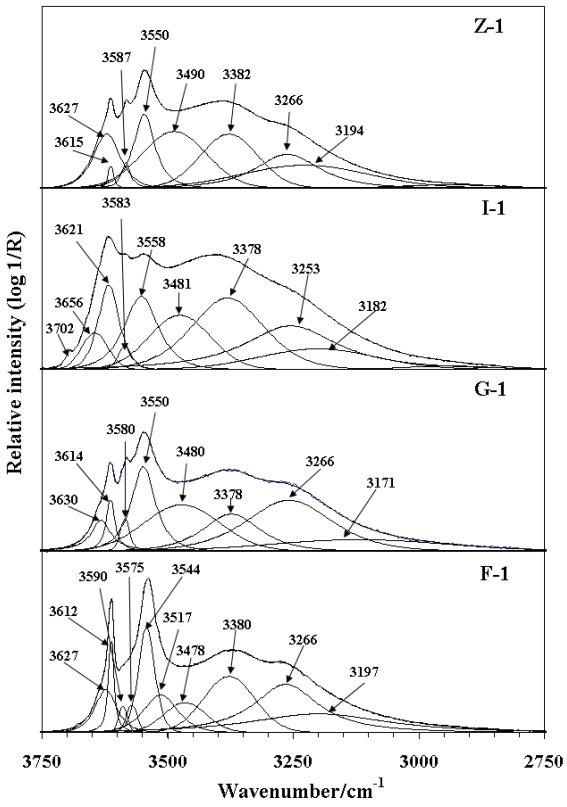
Z-1
3550
3587
3490
3382
3266
3627
3615
3194
I-1
3583
3621
3558
3378
3253
3481
3656
3182
3702
G-1
3550
3580
3614
3480
3266
3630
3378
3171
F-1
3590
3575
3544
3612
3517
3380
3266
3627
3478
3197
Relative intensity (log 1/R)
3750
3500
3250
3000
2750
Wavenumber/cm-1

Fig.3

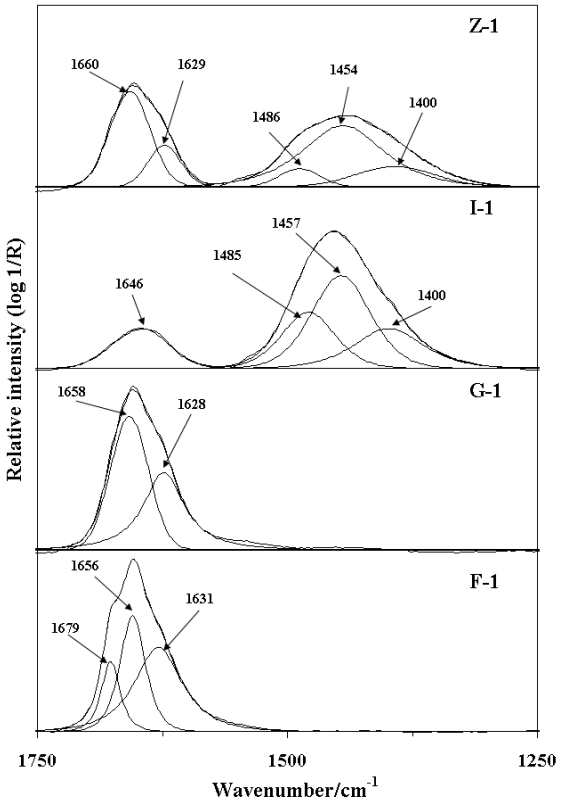
Z-1
1660
1629
1454
1486
1400
I-1
1457
1485
1646
1400
G-1
1658
1628
F-1
1656
1631
1679
Relative intensity (log 1/R)
1750
1500
1250
Wavenumber/cm-1

Fig. 4

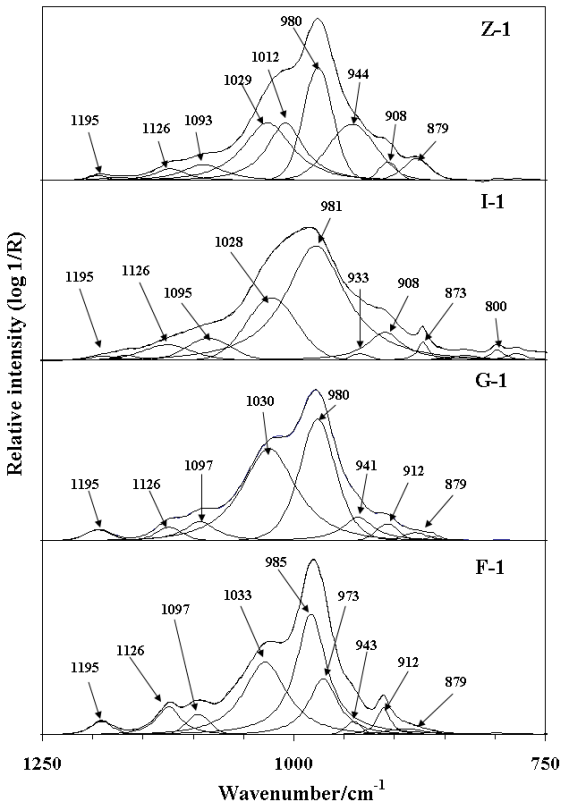
Z-1
980
1012
1029
944
1195
1126
1093
908
879
I-1
981
1028
1195
1126
1095
933
908
873
800
G-1
1030
980
1097
941
912
1195
1126
879
F-1
985
1033
973
1097
1126
943
912
1195
879
Relative intensity (log 1/R)
1250
1000
750
Wavenumber/cm-1

Fig. 5